esa ECOSPHERE

Using LiDAR-derived vegetation metrics for high-resolution, species distribution models for conservation planning

S. L. Farrell,[1,†] B. A. Collier,[1] K. L. Skow,[1] A. M. Long,[2] A. J. Campomizzi,[1] M. L. Morrison,[2] K. B. Hays,[1] and R. N. Wilkins[1,3]

[1]*Texas A&M Institute of Renewable Natural Resources, Texas A&M University, College Station, Texas 77843 USA*
[2]*Department of Wildlife and Fisheries Sciences, Texas A&M University, College Station, Texas 77843-2258 USA*

Citation: Farrell, S. L., B. A. Collier, K. L. Skow, A. M. Long, A. J. Campomizzi, M. L. Morrison, K. B. Hays, and R. N. Wilkins. 2013. Using LiDAR-derived vegetation metrics for high-resolution, species distribution models for conservation planning. Ecosphere 4(3):42. http://dx.doi.org/10.1890/ES12-000352.1

Abstract. Advances in remotely sensed data for characterizing habitat have enabled development of spatially explicit predictive species distribution models (SDM) that can be essential tools for management. SDMs commonly use coarse-grain metrics, such as forest patch size or patch connectivity, over broad spatial extents. However, species distributions are likely driven in part by local, fine-grained habitat conditions. Conservation and management are often planned and applied locally, where coarse predictions may be uninformative or not sufficiently precise. We investigated the integration of high-resolution LiDAR (Light Detection and Ranging) with avian point sampling data to develop a detection-corrected occupancy model to quantify habitat-occurrence relationships for two species with different habitats: the endangered golden-cheeked warbler (*Setophaga chrysoparia*) and black-capped vireo (*Vireo atricapilla*) on a military installation in central Texas. We compared occupancy models that used only the more conventional, coarse remotely sensed metrics to models that also incorporated high-resolution LiDAR-derived metrics for vegetation height and canopy cover, to assess their use for predicting distributions. Models including LiDAR-derived vegetation height and canopy cover metrics were competitive for both species, and models without LiDAR-derived vegetation height had substantially lower model weights and explanatory strength. Area under curve estimates for the highest ranked models were high for warblers (0.864) and moderate for vireos (0.746). Using the best supported models for each species, we predicted the occurrence distribution for both species. The resulting predictions provide a decision support tool that enables assessment of the status, impacts, and mitigation of impacts to endangered species habitat on the installation due to land management and military training activities that is more standardized and accurate than current assessment approaches based on visual gestalt of habitat and expert opinion. Additionally, although previous species distribution models have been created for our focal species, most fail to match the grain and extent of most management actions or include local, fine-grained metrics that influence distributions. In contrast, we demonstrate that use of LiDAR with species occurrence data can provide precision and resolution at a scale that is relevant ecologically and to the operational scale of most conservation and management actions.

Key words: endangered species; habitat occupancy; resource selection; species distribution models.

Received 12 November 2012; revised and accepted 23 January 2013; final version received 28 February 2013; **published** 26 March 2013. Corresponding Editor: J. Thompson.

[3] Present address: East Wildlife Foundation, Corpus Christi, Texas 78411 USA.

† **E-mail:** slfarrell@tamu.edu

Introduction

Species distribution models (SDMs) are important tools for identifying habitats and focusing conservation and management efforts (Guisan and Zimmerman 2000, Austin 2007, Rodriguez et al. 2007). Many SDMs provide general predictions of distribution based on coarse-grain metrics often over broad spatial extents (e.g., patch size) that can reflect coarse patterns of habitat use and provide predictions for broad spatial extents for a variety of conservation and management goals (Betts et al. 2007, Collier et al. 2012). However, habitat use and resulting distributions can be driven by habitat characteristics assessed by organisms at multiple spatial extents and grains, including fine-grained conditions across relatively small spatial extents (Orians and Wittenberger 1991, Meyer and Thuiller 2006, Chalfoun and Martin 2007). Ecological research commonly investigates the role of fine-grained vegetation metrics over small spatial extents when investigating responses such as territory selection or nest site selection (Misenhelter and Rotenberry 2000). Fine-grained metrics, such as vegetation structure and height, are often found to relate to species habitat use and thus may be a useful predictor of species occurrence, but are rarely used to predict species occurrence in a spatially explicit manner (Cody 1981, Wiens et al. 1987, Johnson 2007). However, management is often planned, applied, and monitored over small spatial extents, suggesting the potential utility of fine-grained, spatially explicit occurrence predictions for management planning and decision making.

Numerous studies have investigated habitat-occurrence relationships for the federally endangered golden-cheeked warbler (*Setophaga chrysoparia*; henceforth warbler) and black-capped vireo (*Vireo atricapilla*; henceforth vireo), as habitat loss is considered a threat to population viability for both species (Wilkins et al. 2005, Groce et al. 2010). The breeding ranges of these two species overlap substantially within central Texas, but the species are associated with distinctly different breeding habitats. Warblers are thought to prefer mature mixed oak-juniper (*Quercus* spp.-*Juniperus asheii*) woodlands, with trees ≈4–6 m in height and relatively homogenous closed canopy (Campbell 1996, Ladd and Gass 1999). Vireos, on the other hand, are thought to prefer mid-successional, mixed-species shrub land, with vegetation ≈0.5–3 m in height, moderate percent woody cover with substantial breaks or openings in the woody cover, and vireo habitat is often qualitatively described as being structurally heterogeneous (Grzybowski 1995, Campbell 1996). Across the landscape, warbler and vireo habitat can often be found nearby or directly adjacent to one another within a region (Collier et al. 2012, McFarland et al. 2012*a*). In some cases, habitat that is thought to be suitable for vireos, if left undisturbed, may succeed into the mature woodland used by warblers; conversely, habitat that is actively managed for vireos may prevent succession into potential warbler habitat. Thus, management for these two species can sometimes be viewed as competing, and clearly requires strategic planning if both species are to be effectively managed. Most research on distributions for both species has focused on coarse landscape metrics, such as patch size, patch configuration, and woody cover in the landscape scale (De Boer and Diamond 2006, Magness et al. 2006, Collier et al. 2012) providing a foundation for predicting patterns of warbler distribution at coarse resolutions over broad spatial extents. Efforts have been less successful at prediction of vireo distributions using coarse landscape metrics (McFarland et al. 2012*a*, Wilsey et al. 2012). Given the increasing threat of development within the range of these two endangered species; the extent of efforts to assess impacts and implement management for conservation and restoration; and the potential challenges of managing for two somewhat distinct and potentially competing habitat needs to maintain sufficient habitat and populations, a need for more precise, fine-grain predictions of occurrence is pressing (Wilkins et al. 2005, Groce et al. 2010).

Previous studies suggest vegetation height plays a role in nest site selection, nest success, and foraging activity of many avian species including the warbler and vireo (Dearborn and Sanchez 2001, Bailey and Thompson 2007), though there has been little research investigating vegetation height specifically in relation to occurrence for either species. Where vegetation height has been studied in relation to occurrence or other avian responses, height is typically assessed on the ground. Thus, while studies have long investigated statistical correlations between vegetation height and responses of interest, the technological capacity to estimate height remotely and extrapolate statistical correlations to generate spatially explicit predictions has not been available until more recently (DeBoer and Diamond 2006, McFarland et al. 2012*a*). Previous studies correlating height to avian responses are limited in their ability to be applied to management. For example, studies documenting correlation between a species occurrence and vegetation characteristics as measured on the ground are limited to making general recommendations such as maintaining or protecting areas that are observed to have vegetation of appropriate height. Such studies, in the absence of remotely sensed data with which to associate species response, are unable to provide a platform for remote identification of areas with desirable characteristics or those that could be managed and restored, broad assessment of species distributions, and tools for strategic management planning across a landscape or focal area.

Remotely sensed information on vegetation height is now available via technologies such as LiDAR (Light Detection and Ranging; Hill and Thomson 2005), allowing for precise, high-resolution estimation of numerous descriptors on surface or vegetation structure including vegetation height, and spatially explicit extrapolation of height-based predictions of species distributions (Graf et al. 2009, Seavy et al. 2009, Goetz et al. 2010), which can provide more powerful, effective management tools. Effective management requires an understanding of species occurrence patterns at a scale and resolution that is ecologically and practically relevant. For example, decisions for siting development (e.g., road construction, transmission lines), assessing impacts, mitigation, and management often occur across spatial extents smaller than the grain at which coarse models can distinguish between high and low occupancy areas (McFarland et al. 2012*b*).

Like many military installations, our study area on the Fort Hood military installation provides habitat for wildlife, and management for endangered species conservation is conducted alongside other, sometimes competing, land uses for meeting military training needs (Tazik and Martin 2002, Boice 2006). Fort Hood faces increasing challenges to balance growing military training needs with endangered species conservation and compliance with the Endangered Species Act ([ESA] 1973; Gutzwiller and Hayden 1997, Tazik and Martin 2002). Development projects are often small (e.g., 50 to 100 ha) and locating development can often be adjusted to minimize relative impact to species of concern if the resolution of available data allows. The installation has managed for warbler and vireo since both species were listed in 1987 and 1990, respectively (55 FR 53153, 52 FR 37420). To date, planning decisions on Fort Hood have assumed all areas identified as habitat are equivalent or have relied on qualitative visual assessment and expert opinion of habitat occupancy and quality, limiting the ability to precisely assess impacts and strategically plan. However, even data-driven predictive models of occurrence using coarse habitat metrics would fail to provide the resolution needed to allow strategic management planning and decision making, such as determining where to locate a new airstrip or training range to minimize impacts to the species of concern. Precise, high-resolution predictive models of warbler and vireo distribution and probability of occurrence were necessary to provide improved decision support tools to meet operational and species conservation goals (Fuhlendorf and Smeins 1996, Davenport et al. 2000) and LiDAR data provided one potential tool to move in this direction.

We developed a high-resolution species distribution model for warblers and vireos on Fort Hood military installation using a combination of LiDAR estimation of vegetation height and standard remotely sensed data. While we realize LiDAR can provide a range of metrics that can characterize vegetation structure, we wanted to focus on metrics that had a clear foundation in our ecological understanding of the species (i.e., vegetation height is thought to be important for both species breeding season usage), were reasonably easy to interpret to researchers and resource managers unfamiliar with LiDAR metrics, and provided a starting point for exploring the potential for using more complex structural metrics in the future. We: (1) evaluated whether incorporating LiDAR-derived estimates of vegetation height and canopy cover would provide a more accurate, high-resolution species distribution models than standard remotely sensed spatial metrics alone, and (2) generated a spatially explicit prediction of warbler and vireo distributions as a decision support tool for managing training and conservation goals.

Methods

Study Area

Fort Hood is located in north-central Texas, USA, in the Cross Timbers and Texas Blackland Prairies level III ecoregions (Griffith et al. 2004). Ecoregions are areas with similar ecosystems and environmental resources, delineated as spatial units for research and management. Elevation ranges from 180–375 m above sea level, mean daily high temperatures during the avian breeding season of March to August are 21 to 36°C, and annual rainfall averages 88 cm (National Oceanic and Atmospheric Administration [NOAA]). Vegetation types include pasture, grassland, mixed woodland-shrubland, and mature oak-juniper woodland that includes several deciduous species including Texas or Spanish oak (*Quercus buckleyi*), post oak (*Q. stellata*), and blackjack oak (*Q. marilandica*). Woodland edges, shrubland, and grassland matrices often include young Ashe juniper, shin oak (*Q. sinuata*), redbud (*Cercis Texensis*), false willow (*Baccharis neglecta*), yaupon (*Ilex vomitoria*), and other small woody species, forbs, and grasses. Military training including artillery firing, dismounted and mechanized maneuvers, aircraft gunnery, and aviation training are conducted across the installation. Wildfire is the primary cause of habitat loss for the warbler and vireo on the installation, although brush clearing and prescribed fire is conducted to minimize fuel loads and manage habitat for the vireo (Grzybowski et al. 1994). Our sampling area was the live fire region of Fort Hood, covering about 24,000 ha of the 87,890 ha installation (Fig. 1). Active artillery training is conducted $\approx$ 240 days per year and usually includes use of all or nearly all of the 15 training ranges, using a variety of ordinance from small arms firing ranges to larger ordinance fired into this area from the ground elsewhere on the installation or from aircraft flying over the area. Training aircraft fly over the area frequently and Explosive Ordinance Disposal (EOD) units conduct periodic sweeps to locate and detonate unexploded ordinance across the area.

Sample survey design

We identified all areas with any (>0%) woody cover within the study area using 10 m raster data identifying land cover classification from the Texas Ecological Systems Classification Project (Texas Parks and Wildlife Department 2012) plus a 100 m buffer around the >0% woody cover area as the sampling frame. We erred on the side of being inclusive in the sampling frame, not a priori restricting sampling to areas generally considered habitat for either species (Wilkins et al. 2005, Groce et al. 2010) because recent research indicates habitat use may differ from previous assumptions (Pope 2011, Klassen et al. 2012, Smith et al. 2012). We generated a 300×300 m grid of sample points initiated at a random starting point ($n = 1341$; Thompson 2002). Using standard occupancy model sample size estimators (MacKenzie and Royle 2005) and estimates of probability of detection for both species (Collier et al. 2010, McFarland et al. 2012*b*) and targeting variance of the occupancy estimate at $\leq$6%, we selected a random sample ($n = 453$; Fig. 2) of points. Sampling 453 points across this area resulted in relatively high sampling intensity of approximately one point per 50 ha, which thoroughly covered the study area. We used 100-m fixed radius point sample surveys (Laake et al. 2011); territory sizes of 2 to 4 ha are commonly reported for both species (Grzybowski 1995, Ladd and Gass 1999) making the 3.14 ha sample area biologically appropriate.

Sample survey methods

Two independent observers conducted surveys at the same time and location (MacKenzie 2006, Laake et al. 2011, Collier et al. 2012). For each survey occasion, detection/non-detection histories for each sampling location were 10, 11, 01, or 00 (detected by first observer only, by both observers, by second observer only, or not detected, respectively; MacKenzie and Royle 2005). We visited each point at least two times over one season with most points visited three times, by two independent observers, representing 4–6 detection/non-detection surveys, and we

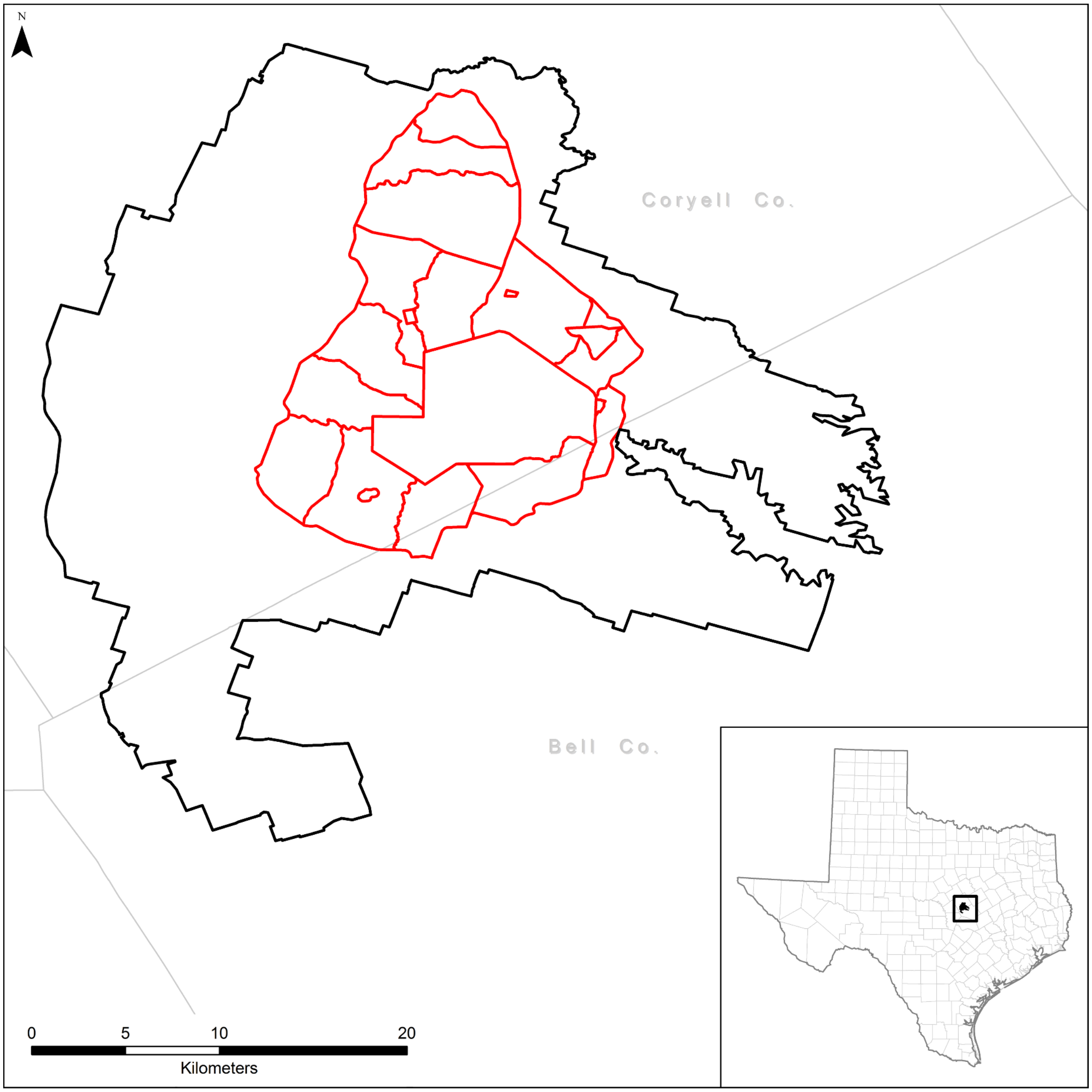

Fig. 1. Texas map with location of Fort Hood military installation in central Texas and zoomed-in view of the Fort Hood military installation with the Live Fire area and live fire training ranges delineated in red, which was surveyed during 2011.

assumed closure (i.e., no immigration or emigration at survey points) within the season (MacKenzie 2006). This assumption is reasonable for these species during the breeding season because both species are territorial. Previous research and monitoring has shown that once individuals establish territories early in the breeding season, the territories remain spatially stable throughout the duration of the season (Lackey et al. 2011, Marshall 2011, Pope 2011, Campomizzi et al. 2012, Farrell et al. 2012, Smith et al. 2012). Observers were randomly allocated to sample locations. Points were sampled from 0600-1200 from 19 March to 16 June 2011 and all repeated surveys were separated by ≥9 days.

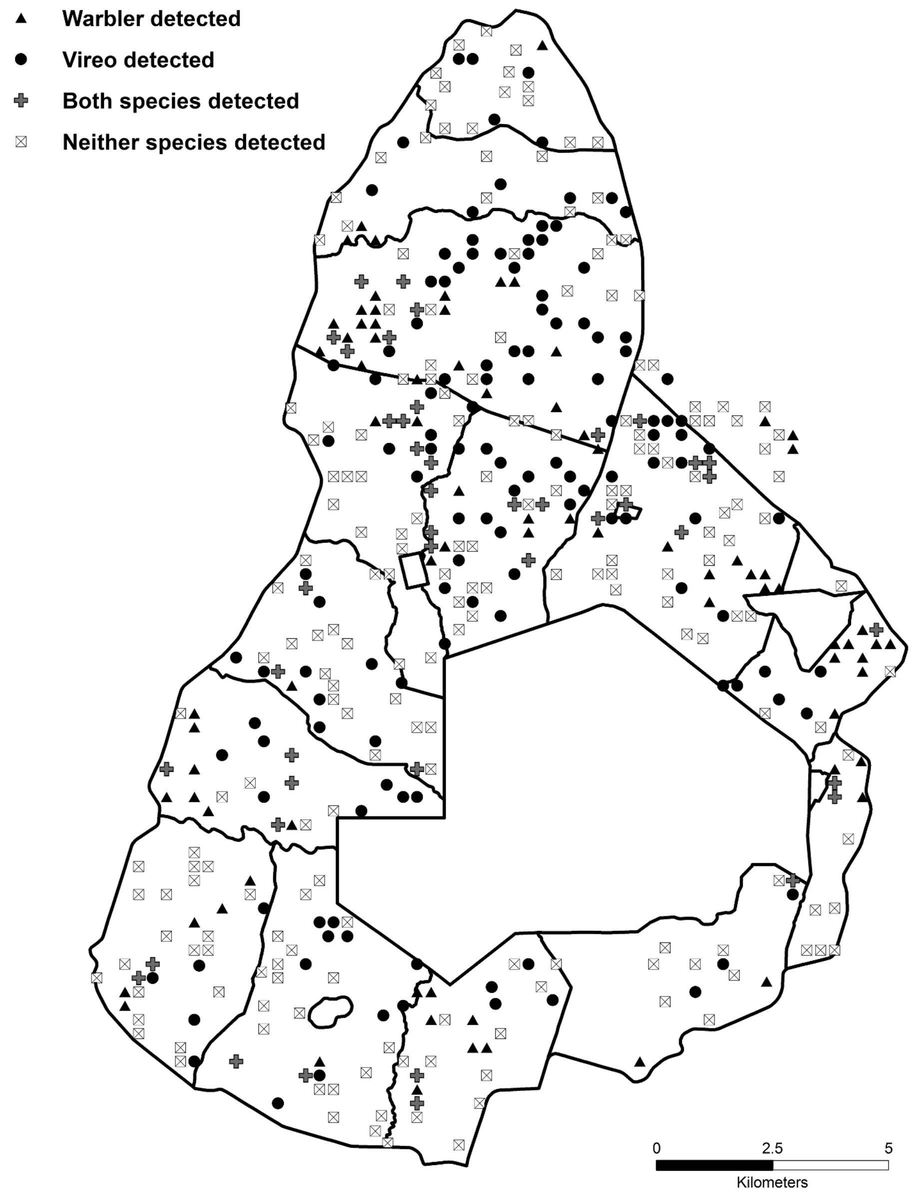

Fig. 2. Point sample locations within the live fire section of the Fort Hood military installation. Points represent the 453 point sample locations sampled in March–July 2011. Color and shape indicate detections at each point: triangle = only warblers were detected, circle = only vireos were detected, cross = both warbler and vireo were detected, open square with "X" = neither species detected.

Remote habitat variable estimation

We used the most current available remotely sensed data for the study area. LiDAR data was acquired 21 to 25 March 2009 (Optimal Geomatics); these data were used to construct the digital surface model (DSM; Applied Imagery Quick Terrain Modeler, Silver Spring, Maryland) for vegetation canopy and the bare earth model ([BEM]; Optimal Geomatics) for the ground level, which together were used to estimate canopy height. Aerial flight elevation was 2200 m above ground level, providing a spot size of 62 cm diameter or 31 cm radius within which each point was located. Average horizontal accuracy was 1/2000 of the flight height giving a horizontal tolerance of <1.1 m. Swath overlap was approximately 30%. Point density was 0.612 returns/m^2. Fundamental vertical accuracy (i.e., in open areas) was 0.47 m and consolidated vertical accuracy (i.e., open terrain, low and high grass, and shrubs and trees) was 0.39 m using root mean squared error (RMSE) $\times$ 1.96. Validation points were used to calculate a consolidated vertical difference of 0.07 m.

We converted first-return LiDAR points (i.e., top heights of the vegetation; Means et al. 1999) into a continuous DSM; we used first returns because we were primarily interested in vegetation height, rather than shape or multi-level structure for this study. We used the BEM model created by Optimal Geomatics to meet the National Map Accuracy Standards ([NMAS] United States Geological Survey) standards for 2 m contours. We set cell resolution for the DSM to 2 m to match the resolution of the BEM. Using a contiguous DSM and BEM we derived the canopy height model (CHM) by subtracting BEM from DSM (Arc10, ESRI, Redlands, California; Lefsky et al. 2002, Popescu et al. 2002). Height values $\geq$35 m were excluded as likely due to errors or returns from non-vegetation sources, such as manmade infrastructure, because trees are typically substantially $<$35 m in the study area. Using the resulting canopy height layer we calculated mean, minimum, maximum, and standard deviation for height within each 100-m point radius.

We used a 2008 aircraft-flown, high-resolution, 3-band, color-infrared SID image taken during leaf-off period and leaf-on imagery to create a layer distinguishing deciduous and evergreen tree species. We resized the 0.35 m resolution to 2 m to match resolution of the LiDAR data. Because we had comprehensive, high-resolution imagery, we did not need to do any additional processing (e.g., smoothing, gap-filling, co-registering the imagery and LiDAR). We classified the image using a k-means unsupervised classification with 50 iterations and no threshold value (ITT Visual Information Solutions ENVI 4.8, Boulder, Colorado; Mather 1999, Duda et al. 2001, Duda and Canty 2002). We used the high-resolution, 3-band, color-infrared leaf-on and leaf-off SID images and vegetation sample data collected in the field to categorize the 20 clusters into corresponding cover types: evergreen, deciduous, mixed, or bare ground and water.

Typical imagery-derived canopy cover estimates include all cover, because height is not easily distinguished and thus including everything from 0.5 m saplings to 10 m trees. However, for our two focal species low woody cover, such as 0.5 m saplings, is not likely serving functionally canopy cover within which they select habitat, for foraging, nesting, or sheltering (Grzybowski 1995, Ladd and Gass 1999, Wilkins et al. 2005, Groce et al. 2010), potentially yielding an estimate of canopy cover that is biased high with regard to what is ecologically relevant to the species. However, in the absence of remote height estimates, it is generally not possible to exclude small saplings and low cover from the shrub or tree canopy data. Because the LiDAR data provided height estimates, we were able to use the CHM (i.e., surface derived using the LIDAR data) to exclude low woody vegetation from the imagery-based estimate of canopy cover. Based on the ecology of the species, we set the cut-off at 1 m (and removed all vegetation $<$1 m tall from the canopy cover data layer). Each 2 m pixel in the resulting data layer was thus characterized as either woody canopy cover $>1 = 1$ or no woody canopy cover >1 m $= 0$. We did not ground-truth this classification; given the high resolution of the data for canopy height and presence of woody canopy cover, it was unlikely that these classes were wrongly assigned to a 2 m cell size.

We used the resulting data layer to calculate percent woody canopy cover. We used a 10-m-radius moving window analysis to assign a percent canopy cover value to each 2 m pixel in the layer (Arc10, ESRI, Redlands, California). We then ran focal statistics for each 100-m-radius point to calculate mean, minimum, maximum, and standard deviation of percent canopy cover within the 100-m-radius. We also used the resulting woody canopy cover- no woody canopy cover layer, in conjunction with the leaf-off and leaf-on imagery, to calculate proportion of evergreen and deciduous cover for each 100-m-radius point.

We calculated the proportion of each ecosite present within each 100 m radius using The Natural Resources Conservation Service (NRCS)

Ecological Site Description (ESD) database. Ecosites are distinctive land type with specific physical characteristics, such as soil and geologic conditions, which influences the potential vegetation assemblages that can emerge there. Recent research has suggested ecosite may influence occurrence for the focal species (Marshall 2011, McFarland et al. 2012*a*).

Distribution modeling

We used a single-season occupancy model with occurrence (ψ) and detection (p) parameters and a suite of species-specific predictive models using metrics we hypothesized would explain warbler and vireo habitat occurrence. We conducted all analyses using the RMark v. 2.1.1 (Laake and Rexstad 2012) interface to MARK (White and Burnham 1999) and developed all map predictions in R 2.15.0 (R Development Core Team 2012). Candidate models included survey day and survey time as covariates for detection as both have been shown to influence warbler and vireo detection rates in Texas (Noa et al. 2007, Collier et al. 2010, Collier et al. 2012). We used an information theoretic approach to model selection and assessed model strength based on Akaike's Information Criterion adjusted for small sample size (AIC_c) and Akaike weights (w_i; Burnham and Anderson 2002).

Using recent work on both species (Collier et al. 2010, Pope 2011, Collier et al. 2012, Farrell et al. 2012, Klassen et al. 2012, McFarland et al. 2012*a*, Smith et al. 2012), we developed candidate models: (1) models including only LiDAR-derived vegetative metrics (Ψ_L), (2) composite models incorporating LiDAR-derived vegetation metrics and non-LiDAR-derived environmental metrics (Ψ_{LC}), and (3) models including only non-LiDAR-derived vegetation and environmental metrics (Ψ_N) (Appendix A: Table A1, Appendix B: Table B1) to determine whether models that included LiDAR-derived metrics were more competitive than those without LiDAR-derived metrics. To create a resource selection surface prediction, we generated a 100-m-radius hexagonal grid over the prediction area from a random starting point. For each grid cell, we estimated the suite of habitat metrics used for occurrence modeling. Based on the best fitting model, we calculated the predicted probability of occupancy for each hexagonal cell creating a resource selection probability surface for occurrence of warblers and vireos across our study site.

We evaluated our model by visualizing a ROC graph showing prediction accuracy versus false-positive rate using our predicted occurrence estimates and our detection/non-detection data. Additionally, we developed a resource selection surface, based on the best fitting models for both the warbler and the vireo, for the entirety of the Fort Hood installation. We compared our mapped predictions with existing habitat delineations for each species generated by visual assessment of imagery and expert opinion of habitat preferences and conditions, which are currently used for management planning on the installation.

Results

We detected warblers at 120 survey locations, vireos at 173 survey locations, and both at 42 of the 453 survey locations (Fig. 2). For both species, detection probability was best explained by models using a covariate for day of season since 15 March 2011, with detection probability declining for warblers but increasing for vireos in concert with the season progressing. Mean detection probability, based on mean survey date (41 days since 19 March), was 0.47 for warblers and 0.38 for vireos. The probability of not detecting a warbler or vireo if it was present at the point sample location and three survey visits were completed by the mean survey date was low: $(1 - 0.47)^6 = 0.02$ for warbler and $(1 - 0.38)^6 = 0.05$ for vireo.

Models that did not include LiDAR-derived vegetation height and canopy cover estimates had substantially lower model weight ($\Delta AIC_c > 50$) than those models that did incorporate LiDAR-derived metrics for canopy cover and height (Appendix A: Table A1, Appendix B: Table B1). For warblers, competitive models incorporated LiDAR-derived metrics for vegetation height and canopy cover; metrics for ecosite were present only in the least competitive of these models ($\Delta AIC_c = 5.78$). Models for warbler that included the LiDAR-derived measure of canopy height but used the typical, not height-corrected, measurement of canopy cover were non-competitive ($\Delta AIC_c \geq 24.07$) compared to those that incorporated LiDAR-corrected estimates of canopy cover (Appendix A: Table A1). For vireos, the only competitive model (w_i = 0.985) was one that incorporated LiDAR-derived vegetation height and LiDAR-corrected canopy cover, in addition to metrics for ecosite (Appendix B: Table B1). The next best, but non-competitive, model given our data (w_i = 0.011) included LiDAR-derived canopy height and conventionally estimated, not height-corrected, measurement of canopy cover (Appendix B: Table B1).

Our model predicted 6329 (26%) of the 24,000 ha in the live fire region with warbler predicted occupancy probabilities $\geq$0.8 (Fig. 3). Predictions for vireos indicated a much wider potential distribution of 4067 ha (17%) with predicted occupancy probability $\geq$0.80, and 23,657 ha (99%) with predicted probabilities >0.50 (Fig. 4). Area under curve estimates for the top model for each species were high for warblers (0.864), and moderate for vireos (0.746) with both indicating our top model predicted reality well. The resource selection surface for both species identified areas currently delineated as habitat as areas with high predicted probability of occurrence based on our model (Figs. 5 and 6), supporting the predictive accuracy of our model when expanded to the area just outside the sampled area.

Discussion

Our results indicate that high-resolution vegetative structure metrics are favorable for identifying species-habitat relationships for both species. Models incorporating LiDAR-derived metrics had higher model weights and were much better supported for predicting occurrence for both species on relatively small units of area than those models which did not include LiDAR-derived metrics. Further, those models which relied on standard methods for estimating canopy cover (e.g., Cunningham and Johnson 2011) but incorporated some LiDAR-derived information for vegetation height were not competitive for warblers ($\Delta AIC_c > 24$) or vireos ($\Delta AIC_c > 8$). Models including traditional canopy cover estimates (e.g., tree cover data) absent any LiDAR-derived metrics were not plausible models ($\Delta AIC_c > 50$) for either species, indicating that standard measures of canopy cover, which have been used to predict warbler distribution at coarser grain and broad spatial extents (Collier et al. 2012), were not as useful for accurate prediction of warbler and vireo distribution at our scale of interest, and the most parsimonious models included LiDAR-derived estimates of local vegetation structure.

Our results demonstrate the value of local, fine-grained vegetative structure metrics for predicting distributions at a scale at which management actions often occur. Although we do not expect all remotely sensed data will describe ecologically relevant habitat characteristics at an ecologically relevant resolution for understanding the habitat use of all species of interest, we found that models including high-resolution structure metrics performed well relative to models using more common, coarsely estimated, remotely sensed metrics for our focal species. Remotely sensed structural data effectively described habitat conditions at a resolution relevant to ecological patterns of bird habitat use for our two focal species that use distinctly different vegetation types. In the case of the vireo, more common approaches using coarse remotely sensed data have failed to produce any published model of the species occurrence, regardless of scale or resolution. Thus, our results provide some new insight into understanding how to describe where vireos occur and may help guide future investigations into why vireos occur where they do. For both species, recent research has suggested that previously assumed habitat relationships may in fact vary across the species' ranges, among years, among individuals, and in the context of various social and behavioral conditions (Pope 2011, Farrell et al. 2012, Klassen et al. 2012, Smith et al. 2012). The capacity to estimate vegetation height and perhaps other structural metrics remotely to relate to species response variables among years, across regions, and even among territories or nest sites can provide an essential tool for developing a more complete and accurate understanding of the habitat associations for these species and provide insight into the mechanisms driving these patterns.

Using quantitative methods for species distribution modeling is an important component of research interested in monitoring status, trends, and impacts to endangered species. Combining

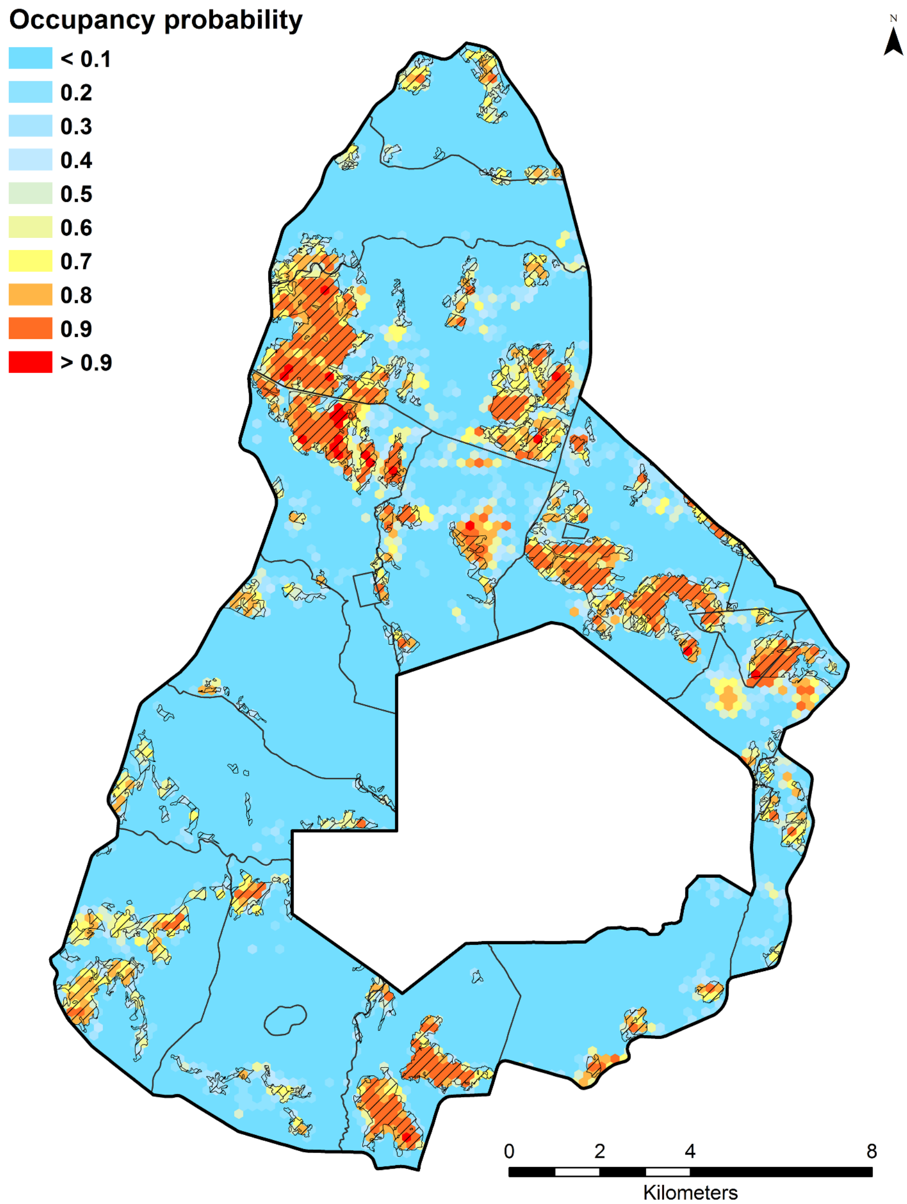

Fig. 3. Occurrence probability predictions for golden-cheeked warbler mapped to the live fire section of the Fort Hood military installation. Diagonal hatched regions represent areas hand delineated (updated November 2011) by Fort Hood staff as golden-cheeked warbler habitat. Probability of occupancy is grouped into categories of <0.1 to >0.9 by 0.1. Occupancy probabilities are color-coded with red indicating highest occupancy probability areas, orange and yellow indicating moderate occupancy probability areas and blue indicating low occupancy probability areas.

avian survey data with LiDAR-derived vegetation data allows for creation of dynamic models (sensu MacKenzie et al. 2003) of avian occurrence and distribution relative to changing habitat conditions. High-resolution, spatially explicit occurrence models that can predict accurately to small units of area, such as ours, can be used to identify and prioritize areas for management; simulate, evaluate, and compare conservation and management planning scenarios (McFarland

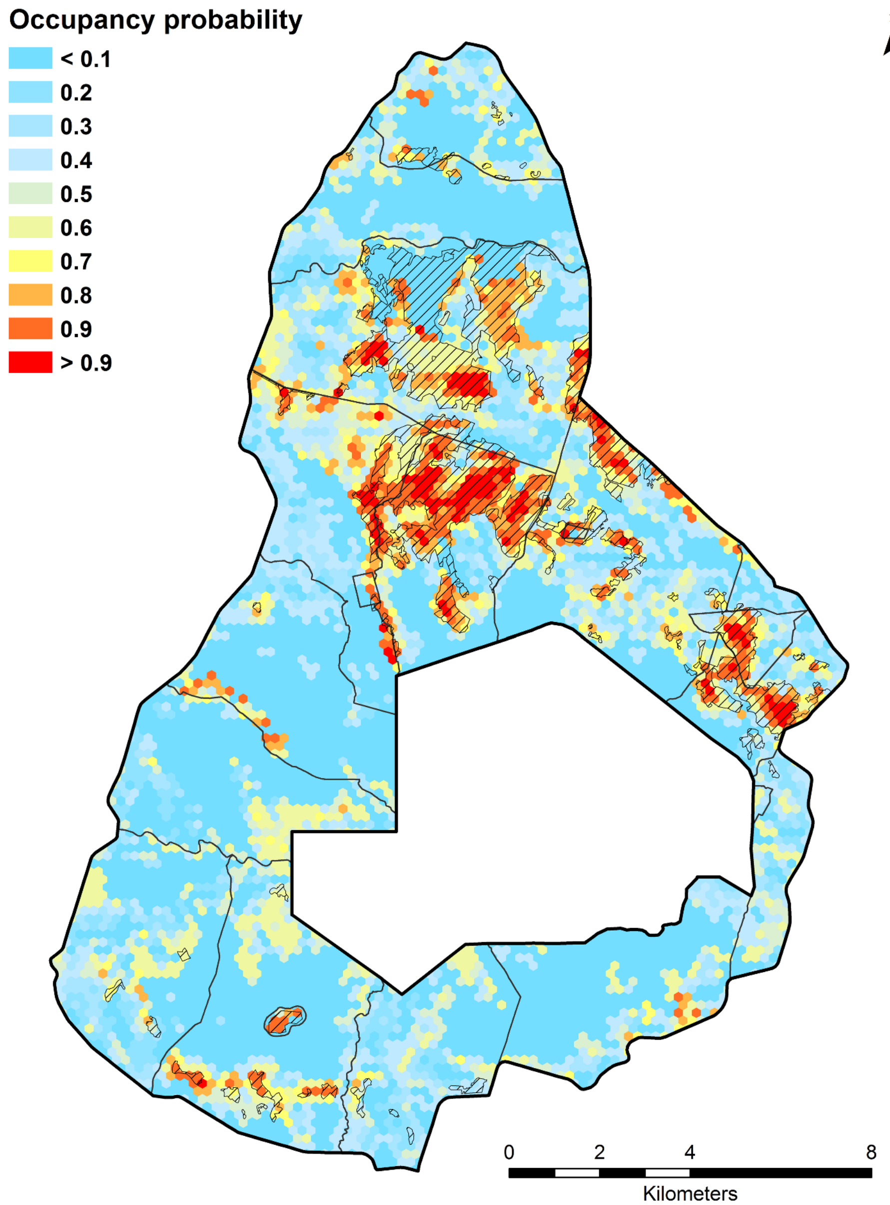

Fig. 4. Occurrence probability predictions for black-capped vireo mapped to the live fire section of the Fort Hood military installation. Diagonal hatched regions represent areas hand delineated (updated November 2011) by Fort Hood staff as black-capped vireo habitat. Probability of occupancy is grouped into categories of <0.1 to >0.9 by 0.1. Occupancy probabilities are color-coded with red indicating highest occupancy probability areas, orange and yellow indicating moderate occupancy probability areas and blue indicating low occupancy probability areas.

et al. 2012*b*); assess and mitigate for impacts, and monitor status and trends at a resolution and extent that is relevant ecologically and practically (Jones 2001, Chalfoun and Martin 2007); and provide decision support for conservation planning and policy development and for adaptive management or other structured decision making processes (Martin et al. 2009).

Identification of habitat for our target species has been the focus of much interest because of its

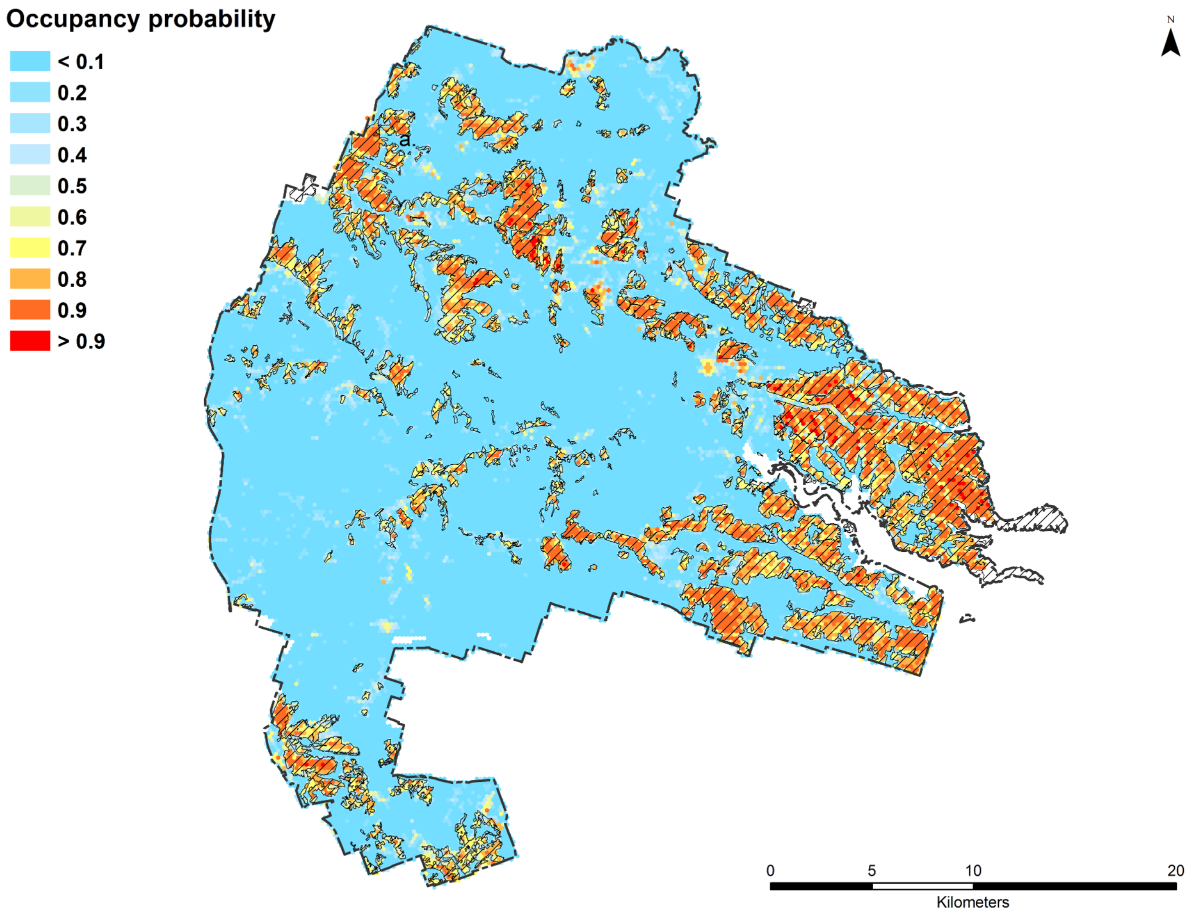

Fig. 5. Mapped predictions from the best fitting occurrence model for golden-cheeked warbler based on data collected within the life fire section of the installation to the entirety of the Fort Hood military installation. Diagonal hatched regions represent areas hand delineated by Fort Hood staff as golden-cheeked warbler habitat. Probability of occupancy is grouped into categories of <0.1 to >0.9 by 0.1. Occupancy probabilities are color-coded with red indicating highest occupancy probability areas, orange and yellow indicating moderate occupancy probability areas, and blue indicating low occupancy probability areas.

use in informing decisions for species conservation and management. Management plans, restoration actions, impact assessment, and mitigation of environmental or anthropogenic impacts are often conducted over small spatial extents, typically within protected areas or small parcels of private lands. Thus, areas where management actions are applied and evaluated are often small relative to the scale and precision of existing occurrence predictions; approaches that identify distribution patterns relative to vegetative conditions with a high-resolution can only increase our ability to predict to small spatial units of area and to increase the effectiveness and efficiency of conservation and management practices (Vierling et al. 2008). Our approach, combining species detection/non-detection data with high-resolution vegetation structure information, provides a high-resolution species distribution model that is standardized and transparent for use in informing future management actions in the context of growing challenges to meet conservation goals, balance multiple land use needs, and track ever-changing environmental and land use conditions.

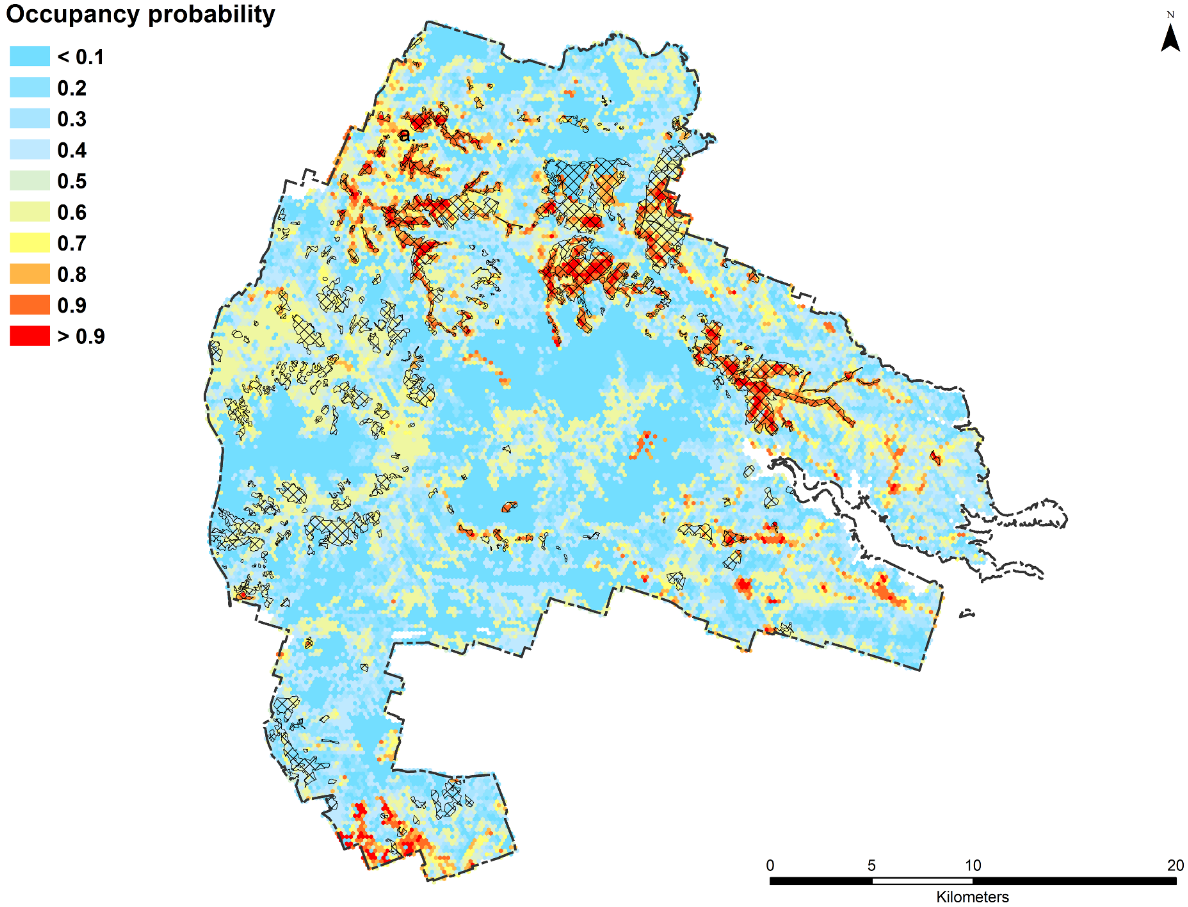

Fig. 6. Mapped predictions from the best fitting occurrence models for black-capped vireo based on data collected within the life fire section of the installation to the entirety of the Fort Hood military installation. Diagonal hatched regions represent areas hand delineated by Fort Hood staff as black-capped vireo habitat. Probability of occupancy is grouped into categories of <0.1 to >0.9 by 0.1. Occupancy probabilities are color-coded with red indicating highest occupancy probability areas, orange and yellow indicating moderate occupancy probability areas, and blue indicating low occupancy probability areas.

Acknowledgments

The US Army Integrated Training Area Management (ITAM) Program, Office of the Secretary of Defense, Department of Defense provided funding support. S. Manning, D. Petty, J. Tatum, and M. Marshall provided additional indispensable logistical and field support. Lastly, we thank field technicians M. Gasner, M. Boone, A. Stuckert, I. Walker, A. Hill, S. Quasius, H. Pruett, A. Connor, J. Hennig, and S. Walters for their efforts and contribution to data collection and management.

Literature Cited

Austin, M. 2007. Species distribution models and ecological theory: a critical assessment and some possible new approaches. Ecological Modeling 200:1–19.

Bailey, J. W. and F. R. Thompson III. 2007. Multiscale nest-site selection by black-capped vireos. Journal of Wildlife Management 71:828–836.

Betts, M. G., G. J. Forbes, and A. W. Diamond. 2007. Thresholds in songbird occurrence in relation to landscape structure. Conservation Biology 21:1046–1058.

Boice, L. P. 2006. Defense and conservation: compatible missions. Endangered Species Bulletin 31:4–7.

Burnham, K. P. and D. R. Anderson. 2002. Model selection and multimodel inference: a practical information-theoretic approach. Springer Verlag, New York, New York, USA.

Campbell, L. 1996. Endangered and threatened animals of Texas—Their life history and management. Texas Parks and Wildlife Press, Austin, Texas, USA.

Campomizzi, A. J., S. L. Farrell, T. M. McFarland, H. A. Mathewson, M. L. Morrison, and R. N. Wilkins. 2012. Species conservation at a broad spatial scale: reproductive success of golden-cheeked warblers across their breeding range. Wildlife Society Bulletin 36:440–449.

Chalfoun, A. D. and T. E. Martin. 2007. Assessments of habitat preferences and quality depend on spatial scale and metrics of fitness. Journal of Applied Ecology 44:983–992.

Cody, M. L. 1981. Habitat selection in birds: the roles of habitat structure, competitors, and productivity. BioScience 31:107–113.

Collier, B. A., M. L. Morrison, S. L. Farrell, A. C. Campomizzi, J. A. Butcher, K. B. Hays, D. I. MacKenzie, and R. N. Wilkins. 2010. Monitoring endangered species occupying private lands: case study using the golden-cheeked warbler. Journal of Wildlife Management 74:140–147.

Collier, B. A., J. E. Groce, M. L. Morrison, J. C. Newnam, A. J. Campomizzi, S. L. Farrell, H. A. Mathewson, R. T. Snelgrove, R. J. Carroll, and R. N. Wilkins. 2012. Predicting patch occupancy in fragmented landscapes at the rangewide scale for an endangered species: an example of an American warbler. Diversity and Distributions 18:158–167.

Cunningham, M. A. and D. H. Johnson. 2011. Seeking parsimony in landscape metrics. Journal of Wildlife Management 75:692–701.

Davenport, I. J., R. R. Bradbury, G. Q. A. Anderson, G. R. F. Hayman, J. R. Krebs, D. C. Mason, J. D. Wilson, and N. J. Veck. 2000. Improving bird population models using airborne remote sensing. International Journal of Remote Sensing 21:2705–2717.

Dearborn, D. and L. Sanchez. 2001. Do golden-cheeked warblers select nets locations on the basis of patch vegetation? Auk 118:1052–1057.

DeBoer, T. S. and D. D. Diamond. 2006. Predicting presence-absence of the endangered golden-cheeked warbler (*Dendroica chrysoparia*). Southwestern Naturalist 51:181–190.

Duda, R. O., P. E. Hart, and D. G. Stork. 2001. Pattern classification. Second edition. John Wiley & Sons, New York, New York, USA.

Duda, T. and M. Canty. 2002. Unsupervised classification of satellite imagery: Choosing a good algorithm. International Journal of Remote Sensing 23:2193–2212.

Farrell, S. L., M. L. Morrison, A. J. Campomizzi, and R. N. Wilkins. 2012. Conspecific cues and breeding habitat selection in an endangered wood warbler. Journal of Animal Ecology 81:1056–1064.

Fuhlendorf, S. D. and F. E. Smeins. 1996. Spatial scale influence on longterm temporal patterns of a semi-arid grassland. Landscape Ecology 11:107–113.

Goetz, S. J., D. Steinberg, M. G. Betts, R. T. Holmes, P. J. Doran, R. Dubayah, and M. Hofton. 2010. Lidar remote sensing variables predict breeding habitat of a Neotropical migrant bird. Ecology 91:1569–1576.

Graf, R. F., L. Mathys, and K. Bollmann. 2009. Habitat assessment for forest dwelling species using LiDAR remote sensing: Capercaillie in the Alps. Forest Ecology and Management 257:160–167.

Groce, J. E., H. A. Mathewson, M. L. Morrison, and R. N. Wilkins. 2010. Scientific evaluation for the 5-year status review of the golden-cheeked warbler. U.S. Fish and Wildlife Service, Region 2, Albuquerque, New Mexico, USA.

Grzybowski, J. A., D. J. Tazik, and G. D. Schnell. 1994. Regional analysis of black-capped vireo breeding habitats. Condor 96:512–544.

Grzybowski, J. A. 1995. Black-capped Vireo (*Vireo atricapillus*). Account 181 *in* A. Poole and F. Gill, editors. The birds of North America. Academy of Natural Sciences, Philadelphia, Pennsylvania. and American Ornithologists' Union, Washington, D.C., USA.

Guisan, A. and N. E. Zimmermann. 2000. Predictive habitat distribution models in ecology. Ecological Modelling 135:147–186.

Gutzwiller, K. J. and T. J. Hayden. 1997. A literature review of actual and potential effects of military maneuvers on avian behavior, reproduction, and community structure. Technical Report 97/98. U.S. Army Construction Engineering Research Laboratories, Champaign, Illinois, USA.

Griffith, G. E., S. A. Bryce, J. M. Omernik, J. A. Comstock, C. Rogers, B. Harrison, S. Hatch, and D. Bezanson. 2004. Ecoregions of Texas. U.S. Geological Survey, Reston, Virginia, USA.

Hill, R. A. and A. G. Thomson. 2005. Mapping woodland species composition and structure using airborne spectral and LiDAR data. International Journal of Remote Sensing 26:3763–3779.

Johnson, M. D. 2007. Measuring habitat quality: a review. Condor 109:489–504.

Jones, J. 2001. Habitat selection studies in avian ecology: a critical review. Auk 118:557–562.

Klassen, J. A., M. L. Morrison, H. A. Mathewson, G. G. Rosenthal, and R. N. Wilkins. 2012. Canopy characteristics affecting reproductive success of golden-cheeked warblers. Wildlife Society Bulletin 36:54–60.

Lackey, M. A., M. L. Morrison, Z. G. Loman, N. Fisher, S. L. Farrell, B. A. Collier, and R. N. Wilkins. 2011. Effects of road construction noise on the endangered golden-cheeked warbler. Wildlife Society Bulletin 35:15–19.

Laake, J. L., B. A. Collier, M. L. Morrison, and R. N. Wilkins. 2011. Point-based mark-recapture distance sampling. Journal of Agricultural, Biological, and Environmental Statistics 16:389–408.

Laake, J. and E. Rexstad. 2012. RMark: R code for MARK analysis. R Package Version 2.1.1. R Foundation for Statistical Computing, Vienna, Austria.

Ladd, C. and L. Gass. 1999. Golden-cheeked warbler (*Dendroica chrysoparia*). Account 420 *in* A. Poole and F. Gill, editors. The birds of North America. The Academy of Natural Sciences, Philadelphia, Pennsylvania. and the American Ornithologists' Union, Washington, D.C., USA.

Lefsky, M. A., W. B. Cohen, G. G. Parker, and D. J. Harding. 2002. Lidar remote sensing for ecosytem studies. BioScience 52:19–30.

MacKenzie, D. I., J. D. Nichols, J. E. Hines, M. G. Knutson, and A. B. Franklin. 2003. Estimating site occupancy, colonization, and local extinction when a species is detected imperfectly. Ecology 84:2200–2207.

MacKenzie, D. I. and J. A. Royle. 2005. Designing occupancy studies: general advice and allocating survey effort. Journal of Applied Ecology 42:1105–1114.

MacKenzie, D. I. 2006. Modeling the probability of resource use: the effect of, and dealing with, detecting a species imperfectly. Journal of Wildlife Management 70:367–374.

Magness, D. R., R. N. Wilkins, and S. J. Hejl. 2006. Quantitative relationships among golden-cheeked warbler occurrence and landscape size, composition, and structure. Wildlife Society Bulletin 34:473–479.

Marshall, M. E. 2011. Effects of tree species composition and foraging effort on the productivity of golden-cheeked warblers. Thesis. Texas A&M University, College Station, Texas, USA.

Martin, J., M. C. Runge, J. D. Nichols, B. C. Lubow, and W. L. Kendall. 2009. Structured decision making as a conceptual framework to identify thresholds for conservation and management. Ecological Applications 19:1079–1090.

Mather, P. M. 1999. Computer processing of remotely-sensed images: An introduction. Second edition. John Wiley & Sons, New York, New York, USA.

McFarland, T. M., H. A. Mathewson, M. L. Morrison, R. T. Snelgrove, J. E. Groce, K. Skow, B. A. Collier, and R. N. Wilkins. 2012*a*. Estimating the distribution and abundance of the black-capped vireo in Texas. Texas A&M Institute of Renewable Natural Resources, College Station, Texas, USA.

McFarland, T. M., H. A. Mathewson, J. E. Groce, M. L. Morrison, C. Newnam, R. T. Snelgrove, K. Skow, B. A. Collier, and R. N. Wilkins. 2012*b*. Utilization of a species distribution model for management and conservation. Wildlife Society Bulletin 36:432–439.

Means, J. E., S. A. Acker, D. J. Harding, J. B. Blair, M. A. Lefsky, W. B. Cohen, M. E. Harmon, and W. A. McKee. 1999. Use of large-footprint scanning airborne Lidar to estimate forest stand characteristics in the Western Cascades of Oregon. Remote Sensing of Environment 67:298–308.

Meyer, C. B. and W. Thuiller. 2006. Accuracy of resource selection functions across spatial scales. Diversity and Distributions 12:288–297.

Misenhelter, M. D. and J. T. Rotenberry. 2000. Choices and consequences of habitat occupancy and nest site selection in sage sparrows. Ecology 81:2892–2901.

National Oceanic and Atmospheric Administration. 1981–2010. Waco: Normals 1981–2010, means, and extremes. National Weather Service, Silver Spring, Maryland, USA. http://www.srh.noaa.gov/fwd/?n=actann

Noa, L. A., D. H. Hirth, T. M. Donovan, and D. Cimprich. 2007. Demographic differences of black-capped vireos in 2 habitat types in central Texas. Journal of Wildlife Management 71:1042–1049.

Orians, G. H. and J. F. Wittenberger. 1991. Spatial and temporal scales in habitat selection. American Naturalist 137:29–49.

Pope, T. L. 2011. Effects of habitat characteristics and adult behavior on black-capped vireo nest and fledgling survival. Dissertation. Texas A&M University, College Station, Texas, USA.

Popescu, S. C., R. H. Wynne, and R. F. Nelson. 2002. Estimating plot-level tree heights with lidar: local filtering with a canopy-height based window size. Computers and Electronics in Agriculture 37:71–95.

Rodriguez, J. P., L. Brotons, J. Bustamante, and J. Seoane. 2007. The application of predictive modelling of species distribution to biodiversity conservation. Diversity and Distributions 13:243–251.

Seavy, N. E., J. H. Viers, and J. K. Wood. 2009. Riparian bird response to vegetation structure: a multiscale analysis using LiDAR measurements of canopy height. Ecological Applications 19:1848–1857.

Smith, K. N., J. W. Cain, M. L. Morrison, and R. N. Wilkins. 2012. Nesting ecology of the black-capped vireo in southwest Texas. Wilson Journal of Ornithology 124:277–285.

Tazik, D. J. and C. O. Martin. 2002. Threatened and endangered species on U.S. Department of Defense lands in the arid west, USA. Arid Land Research and Management 16:259–276.

Texas Parks and Wildlife Department. 2012. Texas ecological systems classification project. https://www.tpwd.state.tx.us/landwater/land/maps/gis/

tescp/index.phtml

Thompson, S. K. 2002. Sampling. Second edition. John Wiley and Sons, New York, New York, USA.

Vierling, K. T., L. A. Vierling, W. A. Gould, S. Martinuzzi, and R. M. Clawges. 2008. Lidar: shedding new light on habitat characterization and modeling. Frontiers in Ecology and the Environment 6:90–98.

Wiens, J. A., J. T. Rotenberry, and B. V. Horne. 1987. Habitat occupancy patterns of North American shrubsteppe birds: the effects of spatial scale. Oikos 48:132–147.

White, G. C. and K. P. Burnham. 1999. Program MARK: survival estimation from populations of marked animals. Bird Study 46:120–138.

Wilkins, R. N., R. A. Powell, A. A. T. Conkey, and A. G. Snelgrove. 2005. Population status and threat analysis for the black-capped vireo. U.S. Fish and Wildlife Service, Region 2, Albuquerque, New Mexico, USA.

Wilsey, C., J. J. Lawler, and D. Cimprich. 2012. Performance of habitat suitability models for the endangered black-capped vireo built with remotely-sensed data. Remote Sensing of Environment 119:35–42.

Supplemental Material

Appendix A

Table A1. Model selection table for candidate models fitted to golden-cheeked warbler occurrence data from point sampling on Ft. Hood, Texas during 2011. Models which rely strictly on LiDAR data were denoted by (Ψ_L), models which rely on a combination of LiDAR and non-LiDAR metrics were denoted by (Ψ_{LC}) and models which rely strictly on non-LiDAR metrics were denoted by (Ψ_N).

Occurrence model	Detection model	k	ΔAIC_c	w_i
Ψ_L(Mean Can cov + Mean Can hght)	p(Day)	5	0†	0.57
Ψ_L(% Decid + % Evergr + Mean Can Hght)	p(Day)	6	1.48	0.27
Ψ_L(Mean Can cov + % Evergr + Min Can Hght + SD Can Hght)	p(Day)	7	4.17	0.07
Ψ_L(% Decid + % Evergr + Min Can Hght)	p(Day)	6	4.97	0.04
Ψ_{LC}(% Decid + % Evergr + Ecosite-LSH + Ecosite-CL + Ecosite-SA)	p(Day)	8	5.78	0.03
Ψ_{LC}(Unadj Mean Can Cov + Mean Can Hght)	p(Day)	5	24.07	<0.01
Ψ_{LC}(Mean Can Cov: Mean Can Hght + Ecosite-LSH + Ecosite-CL + Ecosite-SA)	p(Day)	7	25.99	<0.01
Ψ_L(Mean Can Cov: Mean Can Hght)	p(Day)	7	26.26	<0.01
Ψ_{LC}(Unadj Mean Can Cov + Mean Can Hght)	p(Day)	4	29.65	0
Ψ_{LC}(Mean Can Cov: % Evergr + Mean Can Hght + Ecosite-LSH + Ecosite-SA)	p(Day)	7	30.03	0
Ψ_{LC}(Mean Can Cov: Mean Can Hght)	p(Day)	4	30.69	0
Ψ_{LC}(Mean Can Cov: % Evergr + Mean Can Hght + Ecosite-LSH + Ecosite-CL + Ecosite-SA)	p(Day)	8	31.02	0
Ψ_{LC}(Unadj Mean Can Cov: % Evergr + Mean Can Hght + Ecosite-LSH + Ecosite-SA)	p(Day)	7	31.77	0
Ψ_{LC}(Unadj Mean Can Cov: % Evergr + Mean Can Hght + Ecosite-LSH + Ecosite-CL + Ecosite-SA)	p(Day)	8	32.73	0
Ψ_L(Mean Can Cov:% Evergr + Mean Can Hght)	p(Day)	5	35.61	0
Ψ_{LC}(Unadj Mean Can Cov + % Evergr + Min Can Hght + SD Can Hght)	p(Day)	7	38.33	0
Ψ_{LC}(Unadj Mean Can Cov: % Evergr + Mean Can Hght)	p(Day)	5	38.78	0
Ψ_N(Unadj Mean Can Cov)	p(Day)	4	51.61	0
Ψ_N(Unadj Mean Can Cov + Ecosite-LSH + Ecosite-CL + Ecosite-SA)	p(Day)	7	56.38	0
Ψ_L(Mean Can Cov + Mean Can Hght)	p(Day:Time)	5	60.59	0
Ψ_{LC}(% Decid + % Evergr + Mean Can Hght)	p(Day:Time)	7	60.91	0
Ψ_L(Mean Can Cov + % Evergr + Min Can Hght + SD Can Hght)	p(Day:Time)	7	64.63	0
Ψ_L(% Decid + % Evergr + Min Can Hght)	p(Day:Time)	6	65.39	0
Ψ_{LC}(Mean Can Cov + Ecosite-LSH + Ecosite-CL + Ecosite-SA)	p(Day:Time)	7	65.45	0
Ψ_{LC}(% Decid + % Evergr + Ecosite-LSH + Ecosite-CL + Ecosite-SA)	p(Day:Time)	8	66.01	0
Ψ_{LC}(Unadj Mean Can Cov + Mean Can Hght)	p(Day:Time)	5	84.22	0
Ψ_{LC}(Mean Can Cov: Mean Can Hght + Ecosite-LSH + Ecosite-CL + Ecosite-SA)	p(Day:Time)	7	85.84	0
Ψ_{LC}(Unadj Mean Can Cov: Mean Can Hght + Ecosite-LSH + Ecosite-CL + Ecosite-SA)	p(Day:Time)	7	86.23	0
Ψ_{LC}(Unadj Mean Can Cov: Mean Can Hght)	p(Day:Time)	4	89.13	0
Ψ_{LC}(Mean Can cov: % Evergr + Mean Can Hght + Ecosite-LSH + Ecosite-SA)	p(Day:Time)	7	89.74	0
Ψ_L(Mean Can Cov: Mean Can Hght)	p(Day:Time)	4	90.14	0
Ψ_{LC}(Mean Can Cov: % Evergr + Mean Can Hght + Ecosite-LSH + Ecosite-CL + Ecosite-SA)	p(Day:Time)	8	90.80	0
Ψ_{LC}(Unadj Mean Can Cov: % Evergr + Mean Can Hght + Ecosite-LSH + Ecosite-SA)	p(Day:Time)	7	91.28	0

Table A1. Continued.

Occurrence model	Detection model	k	ΔAIC_c	w_i
Ψ_{LC}(Unadj Mean Can Cov: % Evergr + Mean Can Hght+ Ecosite-LSH + Ecosite-CL + Ecosite-SA)	p(Day:Time)	7	92.33	0
Ψ_{L}(Mean Can Cov: % Evergr + Mean Can Hght)	p(Day:Time)	5	95.12	0
Ψ_{LC}(Unadj Mean Can Cov:% Evergr + Mean Can Hght)	p(Day:Time)	5	98.11	0
Ψ_{L}(% Decid + % Evergr + Min Can Hght + SD Can Hght)	p(Day:Time)	7	99.78	0
Ψ_{LC}(Unadj Mean Can Cov: % Evergr + Ecosite-LSH + Ecosite-CL + Ecosite-SA)	p(Day:Time)	7	>100	0
Ψ_{LC}(Unadj Mean Can Cov:% Evergr)	p(Day:Time)	4	>100	0

Note: Model parameters are: Can Cov: LiDAR derived estimate of canopy cover; Unadj Can Cov: non-LiDAR derived estimate of canopy cover; Can Hght: LiDAR derived estimate of canopy height; % Evergr: percentage of evergreen vegetation; % Decid: percentage of deciduous vegetation; Ecosite: proportion of area within each buffer comprised of each ecosite type (LSH = low stony hill, CL = clay loam, SA = steep adobe).

† −2 log-likelihood for best model: 1082.4103.

Appendix B

Table B1. Model selection table for candidate models fitted to black-capped vireo occurrence data from point sampling on Ft. Hood, Texas during 2011. Models which rely strictly on LiDAR data were denoted by (Ψ_L), models which rely on a combination of LiDAR and non-LiDAR metrics were denoted by (Ψ_{LC}) and models which rely strictly on non-LiDAR metrics were denoted by (Ψ_N).

Occurrence model	Detection model	k	ΔAIC_c	w_i
Ψ_{LC}(Mean Can Cov: Mean Can Hght + Ecosite-LSH + Ecosite-CL + Ecosite-SA + Ecosite-SCL)	p(Day)	8	0†	0.985
Ψ_{LC}(Unadj Mean Can Cov: Mean Can Hght + Ecosite-LSH + Ecosite-CL + Ecosite-SA + Ecosite-SCL)	p(Day)	8	9.14	0.011
Ψ_{LC}(Mean Can Cov: Mean Can Hght + Ecosite-LSH + Ecosite-CL)	p(Day)	6	11.60	<0.01
Ψ_{LC}(Mean Can Cov: Mean Can Hght + Ecosite-LSH: Can Hght + Ecosite-CL: Can Hght + Ecosite-SA: Can Hgh + Ecosite-SCL: Can Hght)	p(Day)	8	12.44	<0.01
Ψ_{LC}(Unadj Mean Can Cov: Mean Can Hght + Ecosite-LSH + Ecosite-CL)	p(Day)	6	21.07	0
Ψ_{LC}(Unadj Mean Can Cov: Mean Can Hght + Ecosite-LSH: Can Hght + Ecosite-CL: Can Hght + Ecosite-SA)	p(Day)	8	22.25	0
Ψ_{LC}(Unadj Mean Can Cov: Mean Can Hght)	p(Day)	5	28.18	0
Ψ_{L}(% Evergr + Mean Can Hght)	p(Day)	5	40.16	0
Ψ_{L}(Mean Can Cov + Mean Can Hght)	p(Day)	5	43.45	0
Ψ_{LC}(%Evergr: SD Can Hght + Ecosite-LSH + Ecosite-CL + Ecosite-SA + Ecosite-SCL)	p(Day)	8	45.16	0
Ψ_{N}(Unadj Mean Can Cov + Ecosite-LSH + Ecosite-CL + Ecosite-SA + Ecosite-SCL)	p(Day)	8	51.20	0
Ψ_{LC}(Mean Can Cov + Mean Can Hght: Ecosite-LSH + Ecosite-CL + Mean Can Hght: Ecosite-SA)	p(Day)	7	53.36	0
Ψ_{N}(Unadj Mean Can Cov + Ecosite-LSH + Ecosite-CL)	p(Day)	6	56.63	0
Ψ_{L}(Mean Can Cov: Mean Can Hght)	p(Day)	4	59.97	0
Ψ_{N}(Unadj Mean Can Cov: Ecosite-LSH + Unadj Mean Can Cov: Ecosite-CL)	p(Day)	5	61.42	0
Ψ_{LC}(% Decid: Max Can Cov + Mean Can Hght)	p(Day)	5	67.08	0
Ψ_{LC}(Unadj Mean Can Cov: Mean Can Hght)	p(Day)	4	67.13	0
Ψ_{LC}(Mean Can Cov + Mean Can Hght: Ecosite-LSH + Mean Can Hght: Ecosite-SA)	p(Day)	6	67.78	0
Ψ_{L}(% Decid: Max Can Cov + Max Can Hght)	p(Day)	5	68.31	0
Ψ_{L}(Mean Can Cov: SD Can Hght)	p(Day)	4	69.65	0
Ψ_{LC}(Mean Can Cov: Ecosite-LSH + Mean Can Cov: Ecosite-CL)	p(Day)	5	70.95	0
Ψ_{LC}(Unadj Mean Can Cov + Mean Can Hght: Ecosite-LSH + Mean Can Hght: Ecosite-SA + Ecosite-CL)	p(Day)	7	74.27	0
Ψ_{L}(% Evergr: Mean Can Hght)	p(Day)	4	75.09	0
Ψ_{LC}(Unadj Mean Can Cov: Max Can Hght)	p(Day)	4	78.99	0
Ψ_{L}(% Evergr: SD Can Hght)	p(Day)	4	79.88	0
Ψ_{LC}(Unadj Mean Can Cov: SD Can Hght)	p(Day)	4	81.94	0
Ψ_{N}(Unadj Mean Can Cov)	p(Day)	4	82.43	0
Ψ_{L}(% Evergr: Max Can Cov)	p(Day)	4	83.49	0
Ψ_{LC}(Unadj Mean Can Cov + Mean Can Hght: Ecosite-LSH + Mean Can Hght: Ecosite-SA)	p(Day)	6	84.12	0

Table B1. Continued.

Occurrence model	Detection model	k	ΔAIC_c	w_i
Ψ_{LC}(Mean Can Cov: Mean Can Hght + Ecosite-LSH + Ecosite-CL + Ecosite-SA)	p(Day:Time)	7	91.29	0
Ψ_{LC}(Mean Can Cov: Mean Can Hght + Ecosite-LSH + Ecosite-CL)	p(Day:Time)	6	98.60	0
Ψ_{LC}(Unadj Mean Can Cov: Mean Can Hght + Ecosite-LSH + Ecosite-CL + Ecosite-SA)	p(Day:Time)	7	>100	0
Ψ_{LC}(Unadj Mean Can Cov: Mean Can Hght + Ecosite-LSH + Ecosite-CL)	p(Day:Time)	6	>100	0
Ψ_{LC}(Unadj Mean Can Cov + Mean Can Hght)	p(Day:Time)	5	>100	0
Ψ_{L}(% Evergr + Mean Can Hght)	p(Day:Time)	5	>100	0
Ψ_{LC}(% Evergr: SD Can Hght + Ecosite-LSH + Ecosite-CL + Ecosite-SA + Ecosite-SCL)	p(Day:Time)	8	>100	0
Ψ_{L}(Mean Can Cov + Mean Can Hght)	p(Day:Time)	5	>100	0
Ψ_{N}(Unadj Mean Can Cov + Ecosite-LSH + Ecosite-CL + Ecosite-SA)	p(Day:Time)	7	>100	0
Ψ_{LC}(Mean Can Cov + Mean Can Hght: Ecosite-LSH + Mean Can Hght: Ecosite-SA + Ecosite-CL)	p(Day:Time)	7	>100	0
Ψ_{N}(Unadj Mean Can Cov + Ecosite-LSH + Ecosite-CL)	p(Day:Time)	6	>100	0
Ψ_{LC}(Unadj Mean Can Cov: Ecosite-LSH + Unadj Mean Can Cov: Ecosite-CL)	p(Day:Time)	5	>100	0
Ψ_{L}(Mean Can Cov: Mean Can Hght)	p(Day:Time)	4	>100	0
Ψ_{LC}(Mean Can Cov + Mean Can Hght: Ecosite-LSH + Mean Can Hght: Ecosite-SA)	p(Day:Time)	6	>100	0
Ψ_{L}(Mean Can Cov: Max Can Hght)	p(Day:Time)	4	>100	0
Ψ_{L}(% Decid: Max Can Cov + Mean Can Hght)	p(Day:Time)	5	>100	0
Ψ_{LC}(Unadj Mean Can Cov: Mean Can Hght)	p(Day:Time)	4	>100	0
Ψ_{L}(Mean Can Cov: Ecosite-LSH + Mean Can Cov: Ecosite-CL)	p(Day:Time)	4	>100	0
Ψ_{L}(% Decid: Max Can Cov + Max Can Hght)	p(Day:Time)	5	>100	0
Ψ_{L}(Mean Can Cov: SD Can Hght)	p(Day:Time)	4	>100	0
Ψ_{LC}(Unadj Mean Can Cov + Mean Can Hght: Ecosite-LSH + Mean Can Hght: Ecosite-SA + Ecosite-CL)	p(Day:Time)	7	>100	0
Ψ_{L}(% Evergr: Mean Can Cov)	p(Day:Time)	4	>100	0
Ψ_{LC}(Unadj Mean Can Cov: Max Can Hght)	p(Day:Time)	4	>100	0
Ψ_{LC}(% Evergr: SD Can Hght)	p(Day:Time)	4	>100	0
Ψ_{LC}(Unadj Mean Can Cov: SD Can Hght)	p(Day:Time)	4	>100	0
Ψ_{LC}(Unadj Mean Can Cov + Mean Can Hght: Ecosite-LSH + Mean Can Hght: Ecosite-SA	p(Day:Time)	6	>100	0
Ψ_{LC}(%Evergr: Max Can Hght)	p(Day:Time)	4	>100	0

Note: Model parameters are: Can Cov: LiDAR derived estimate of canopy cover; Unadj Can cov: non-LiDAR derived estimate of canopy cover; Can hght: LiDAR derived estimate of canopy height; % Evergr: percentage of evergreen vegetation; % Decid: percentage of deciduous vegetation; Ecosite: proportion of area within each buffer comprised of each ecosite type (LSH = low stony hill, CL = clay loam, SA = steep adobe, SCL = stony clay loam).

† −2 log-likelihood for best model: 1507.3053.

Supplement

R package (Windows and cross-platform) including all data and analysis (*Ecological Archives* C004-005-S1).